Translational Oncology 14 (2021) 101236

Contents lists available at ScienceDirect

Translational Oncology

journal homepage: www.elsevier.com/locate/tranon

Original Research

Crosstalk between oral squamous cell carcinoma cells and cancer-associated fibroblasts via the TGF-β/SOX9 axis in cancer progression

Kenta Haga [a,b,c], Manabu Yamazaki [c], Satoshi Maruyama [c], Masami Kawaharada [b,c], Ayako Suzuki [a], Emi Hoshikawa [a], Nyein Nyein Chan [b,c], Akinori Funayama [b], Toshihiko Mikami [b], Tadaharu Kobayashi [b], Kenji Izumi [a,*], Jun-ichi Tanuma [c,*]

[a] Division of Biomimetics, Faculty of Dentistry & Niigata University Graduate School of Medical and Dental Sciences, Niigata 951-8514, Japan
[b] Division of Reconstructive Surgery for Oral and Maxillofacial Region, Faculty of Dentistry & Niigata University Graduate School of Medical and Dental Sciences, Niigata 951-8514, Japan
[c] Division of Oral Pathology, Faculty of Dentistry & Niigata University Graduate School of Medical and Dental Sciences, 2-5274 Gakkocho-dori, Chuo-ku, Niigata 951-8514, Japan

ARTICLE INFO

Keywords:
Oral squamous cell carcinoma
CAFs
TGF-β
SOX9
3D *in vitro* model

ABSTRACT

Cancer-associated fibroblasts (CAFs) have important roles in promoting cancer development and progression. We previously reported that high expression of sex-determining region Y (SRY)-box9 (SOX9) in oral squamous cell carcinoma (OSCC) cells was positively correlated with poor prognosis. This study developed three-dimensional (3D) *in vitro* models co-cultured with OSCC cells and CAFs to examine CAF-mediated cancer migration and invasion *in vitro* and *in vivo*. Moreover, we performed an immunohistochemical analysis of alpha-smooth muscle actin and SOX9 expression in surgical specimens from 65 OSCC patients. The results indicated that CAFs promote cancer migration and invasion in migration assays and 3D *in vitro* models. The invading OSCC cells exhibited significant SOX9 expression and changes in the expression of epithelial–mesenchymal transition (EMT) markers, suggesting that SOX9 promotes EMT. TGF-β1 signalling inhibition reduced SOX9 expression and cancer invasion *in vitro* and *in vivo*, indicating that TGF-β1-mediated invasion is dependent on SOX9. In surgical specimens, the presence of CAFs was correlated with SOX9 expression in the invasive cancer nests and had a significant impact on regional recurrence. These findings demonstrate that CAFs promote cancer migration and invasion via the TGF-β/SOX9 axis.

Introduction

Lip, oral cavity and pharynx cancers represent the seventh most common malignancies worldwide. Each year, over 600,000 new cases are diagnosed, and over 300,000 patients die of these disease [1,2]. Most patients are at a high risk of local recurrence and regional and distant metastases, despite radical resection of the primary oral squamous cell carcinoma (OSCC) lesion [3,4]. Thus, it is necessary to understand the mechanism of local invasion, develop more effective therapeutic approaches, and identify markers that predict prognosis.

Cancer tissues consist of both neoplastic parenchymal cells and stromal components including fibroblasts, immune cells, endothelial cells, various secreted growth factors/chemokines, and extracellular matrix proteins. The environment surrounding a tumour is collectively termed the tumour microenvironment (TME), which promotes cancer progression and extracellular matrix remodelling, neoangiogenesis, and tumour growth [5,6]. Cancer-associated fibroblasts (CAFs) are a major cellular component of the cancer stroma in the TME [7,8]. The specific growth factors/cytokines produced by CAFs induce epithelial–mesenchymal transition (EMT) in cancer cells via a paracrine system [9–11]. Alpha-smooth muscle actin (α-SMA) and fibroblast-activated protein are markers of CAFs in many cancers, and a

Abbreviations: CAFs, cancer-associated fibroblasts; CIS, carcinoma in situ; CM, conditioned medium; ELISA, enzyme-linked immunosorbent assay; EMT, epithelial–mesenchymal transition; NOFs, normal oral fibroblasts; OED, oral epithelial dysplasia; OSCC, oral squamous cell carcinoma; SOX9, sex-determining region Y (SRY)-box9; siRNA, short interfering RNA; 3D, three-dimensional; TGF-β, transforming growth factor-β; TME, tumour microenvironment; α-SMA, alpha-smooth muscle actin.

* Corresponding authors.
E-mail addresses: izumik@dent.niigata-u.ac.jp (K. Izumi), tanuma@dent.niigata-u.ac.jp (J.-i. Tanuma).

https://doi.org/10.1016/j.tranon.2021.101236
Received 14 July 2021; Received in revised form 7 September 2021; Accepted 1 October 2021

large number of CAFs in cancer stroma is associated with poor clinical outcomes in various cancers [12,13].

Sex-determining region Y (SRY)-box9 (SOX9) is a transcription factor located in the nucleus that regulates cell fate during male sexual organ development and chondrocyte differentiation [14]. Recent studies have demonstrated that high SOX9 expression in cancer cells correlates with poor outcomes in patients with various cancers [15–17]. For example, in non-small cell lung cancer macrophages infiltrating into the cancer stroma promote SOX9 expression in cancer cells through the transforming growth factor-β (TGF-β) signalling pathway. Both the high density of macrophages and SOX9 expression are associated with poor prognosis [15]. We recently conducted a histological investigation of SOX9 expression levels in patients with OSCC and demonstrated a correlation between SOX9 expression and poor clinical outcomes [18]. However, the interaction between CAFs and cancer cells through the TGF-β/SOX9 axis has not been thoroughly investigated, especially in OSCC.

Three-dimensional (3D) cell culture is considered to be more suitable for mimicking primary tumours compared with traditional two-dimensional (2D) cell cultures [19]. As 3D models mimic the morphological and intrinsic molecular properties and the local microenvironment *in vivo*, they may be more predictive of physiological cell behavior than conventional 2D culture systems [19,20]. We previously established a system for oral mucosa tissue engineering to investigate pathophysiological lesions specific to the oral cavity. This system provides a biomimetic 3D *in vitro* model containing OSCC cells and CAFs [21].

We hypothesised that soluble factors secreted from CAFs, specifically TGF-β, regulate SOX9 expression in OSCC. Therefore, we investigated the role of the TGF-β/SOX9 axis in CAFs and OSCC cells in promoting cancer progression *in vitro* and *in vivo*. We confirmed that the presence of α-SMA-positive CAFs in the cancer stroma was correlated with the clinical outcome in OSCC patients and explored the mechanisms of cancer invasiveness and clues to develop novel therapies.

Materials and methods

Cell lines and CAFs

Human cell lines derived from OSCC, including Ca9-22 (RRID: CVCL_1102), HSC-2 (RRID: CVCL_1287), HSC-3 (RRID: CVCL_1288), and HSC-4 (RRID: CVCL_1289) cell lines, were obtained from the Riken BRC Cell Bank (Tsukuba, Japan). All human cell lines were authenticated using short tandem repeat profiling in May 2020 and all experiments were performed with mycoplasma-free cells. Ca9-22 and HSC-2 are well-differentiated OSCC cell lines, which were established from the primary sites of gingival and oral floor cancer, respectively [22,23]. HSC-3 and HSC-4 are poorly-differentiated and well-differentiated OSCC cell lines, respectively, which were both established from a metastatic lymph node of a tongue cancer [23]. CAFs derived from non-small cell lung cancer were obtained from Cellular Engineering Technologies, Inc. (Coralville, IA, USA). The cells were maintained in Dulbecco's Modified Eagle Medium (DMEM; Thermo Fisher Scientific, Waltham, MA, USA) supplemented with 10% foetal bovine serum (FBS; Corning, New York, NY, USA), gentamicin (5.0 μg/mL), and amphotericin B (0.375 μg/mL; Thermo Fisher Scientific) under a humidified atmosphere of 5% CO_2 at 37 °C. CAFs from passages 3 to 5 were used in the experiments.

The protocol to obtain human oral mucosa tissue samples was approved by the Niigata University Hospital Internal Review Board (2015–5018). Human oral mucosa samples were obtained from patients who received minor dentoalveolar surgery. The patients were provided sufficient information regarding this study, and all participating individuals signed an informed consent form. Primary normal oral fibroblasts (NOFs) were established using an explant culture technique and were serially cultured as previously described [21]. NOFs from passages 3 to 5 were used in the study as a control.

Surgical specimens

Primary OSCC surgical specimens were obtained from 65 OSCC patients who had undergone ablative surgeries at Niigata University Medical & Dental Hospital. The protocol to analyse the surgical materials was approved by the Internal Review Board of Niigata University Medical & Dental Hospital (2018–0228). The clinical stage was determined in accordance with the Union for International Cancer Control TNM classification system, 8th edition [24]. Three pathologists reviewed all paraffin sections, and representative sections were selected that contained the invasive front of OSCC and oral mucosal epithelium showing either intact, oral epithelial dysplasia (OED), or carcinoma in situ (CIS) foci. OSCC was histopathologically graded in accordance with the mode of invasion classification proposed by Jakobsson et al. [25]. The selected sections were cut and prepared for further analysis by Hematoxylin-Eosin (H-E) and immunohistochemical staining.

Generation of the 3D in vitro model of OSCC cells

Collagen matrix solution (Nitta gelatin, Osaka, Japan) containing 5.0×10^5 CAFs or NOFs in a 6-well tissue culture insert (Greiner Bio, Roskilde, Denmark) was incubated with DMEM containing 10% FBS under a humidified atmosphere of 5% CO_2 at 37 °C for 2 days. The composite of collagen matrices was then detached from the wall of the tissue culture insert using a 200-μL micropipette tip. After 5 days, OSCC cells (5.0×10^5 cells) were seeded on the top surface of the collagen matrices. The constructs comprising CAF- or NOF-embedded or acellular collagen matrices (stromal layer) and the overlying OSCC cells were cultured under submerged culture conditions for an additional 7 days [21]. The models were referred to as the 3D cancer-CAF model, the 3D cancer-NOF model, and the 3D cancer-alone model, respectively. Depending on the subsequent assays, the two-layered constructs were then raised to an air–liquid interface and cultured for an additional 7 days. When the models were completed after culturing for 14 or 21 days, they were fixed in 4% paraformaldehyde and embedded in paraffin. The sections were histopathologically and immunohistochemically analysed. All 3D *in vitro* models were independently established three times ($n = 3$).

In some experiments, the stromal layers containing NOFs or CAFs were pre-treated with SB431542 dissolved in dimethyl sulfoxide (1 μM or 10 μM) for 7 days, followed by the seeding of OSCC cells onto the top surface of the stroma. In other experiments, OSCC cells were transfected with short interfering RNA (siRNA) for SOX9 or negative control siRNA using Lipofectamine RNAi MAX (Thermo Fisher Scientific), as described in the supplementary methods. The transfected OSCC cells (5.0×10^5 cells/50 μL) were seeded onto the top surface of the stromal layers containing CAFs. All 3D cancer-CAF models were cultured under submerged conditions with DMEM containing 10% FBS for 7 days.

Statistical analysis

The data are presented as means ± standard deviation (S.D.). The statistical differences were compared by one-way analysis of variance or Fisher's exact test. The Kaplan–Meier method was used for survival analysis (disease-specific survival and relapse-free survival), and the statistical difference was evaluated using the log-rank test. A p-value of less than 0.05 was considered statistically significant.

Supplementary data

Antibodies and reagents [26], immunofluorescence [18], TGF-β1 enzyme-linked immunosorbent assay (ELISA), 2D migration assay, MTT cell viability assay, western blot analysis [27], siRNA transfection, evaluation of the depth of invasion and invasion index in 3D cancer-CAF and cancer-NOF models [28], xenograft models, immunohistochemistry and evaluation of the localisation of CAFs and SOX9 expression in

surgical specimens were available in the supplementary materials and methods.

Results

CAF-derived CM promotes the migration of OSCC cells under 2D cell culture conditions

To confirm that α-SMA and TGF-β1 can be used as putative markers for CAFs in the cancer stroma, we first investigated α-SMA and TGF-β1 expression in CAFs and NOFs under 2D cell culture conditions. Immunopositivity of α-SMA and TGF-β1 was higher in CAFs than in NOFs (Fig. 1A). ELISA revealed that the concentration of TGF-β1 in the culture supernatants (conditioned medium, CM) from the CAFs (CAF-CM) was five times higher than that in NOF-CM and was statistically significant ($p < 0.01$) (Fig. 1B).

Next, we examined the effect of soluble factors secreted from CAFs on the cell migration of OSCC cells using a 2D migration assay. Compared with DMEM or NOF-CM, CAF-CM significantly promoted the migration of all four OSCC cell lines (Fig. 1C and D). Of these, the migration of HSC-3 cells in response to CAF-CM was remarkable because the cell-free area was completely closed within 10 h. Furthermore, SB431542, a specific inhibitor of the TGF-β1 receptor, abolished the pro-migratory effects of CAF-CM (Fig. 1C and D), but did not alter cell viability (Fig. 1E). These findings indicate that CAF-derived TGF-β1 promotes the migration of OSCC cells.

The expression levels of SOX9, p-SMAD2, and SMAD2/3 were evaluated by western blot analysis to investigate the effect of TGF-β1 on SOX9 expression in OSCC cells through the SMAD pathway. SOX9 expression was increased in all four OSCC cell lines in response to TGF-β1 treatment, and the SMAD pathway was also activated in all four OSCC cell lines, although the degree of activation varied (Fig. 1F). These results indicate that TGF-β1 increases SOX9 expression through the SMAD pathway.

CAFs promote cancer invasion in the 3D in vitro models

Histological analysis showed that OSCC cells invaded into the underlying cancer stromal layer in the 3D cancer-CAF models (Fig. 2A). In contrast, high numbers of invasive OSCC cells into the underlying stroma were not detected in the 3D cancer-NOF models or the 3D cancer-alone models. For all OSCC cell lines, both the depth of invasion and the invasion index in the 3D cancer-CAF models were significantly greater compared with those in the 3D cancer-NOF models and 3D cancer-alone models ($p < 0.01$) (Fig. 2B and C). HSC-3 cells exhibited the most prominent invasion of all OSCC cell lines. Our results indicate that CAFs promote the invasiveness of OSCC cells.

SOX9 expression is upregulated in invading OSCC cells by CAFs

We examined the characteristics of 3D *in vitro* models by immunohistochemistry. The invading OSCC cells in the 3D cancer-CAF models showed upregulated SOX9 expression, particularly at the invading front, compared with the non-invading OSCC cells in the 3D cancer-NOF models (Fig. 2D and E).

TGF-β plays an important role in facilitating cancer invasion and may induce EMT [29]. Therefore, we examined the expression levels of EMT markers, such as E-cadherin (a cell attachment marker), vimentin, fibronectin (mesenchymal cell markers) and TWIST2 (an EMT-related transcription factor) at the invading front of the 3D cancer-CAF model using HSC-3 cells (3D HSC-3-CAF model). The expression levels of vimentin, fibronectin and TWIST2 were upregulated in the invading HSC-3 cells, whereas E-cadherin expression was downregulated (Fig. 2F). On the basis of these findings, we confirmed that our 3D cancer-CAF models could possess a specific TME that confers an EMT-like phenotype in OSCC cells.

Inhibition of the TGF-β/SOX9 axis suppresses cancer progression

Our 3D cancer-CAF models can be used as simple and effective tools to study cancer invasion via the TGF-β/SOX9 axis. Therefore, we conducted specific functional assays using the 3D HSC-3-CAF model that demonstrated the most invasiveness. We confirmed that SB431542 decreased SOX9 expression in HSC-3 cells at 1 and 10 μM under 2D cell culture conditions (Fig. 3A). SB431542 also suppressed cancer invasion in the 3D HSC-3-CAF model, in which SOX9 expression was also reduced (Fig. 3B). Both the depth of invasion and the invasion index were markedly diminished in response to SB431542 in a dose-dependent manner (Fig. 3C and D). However, we considered the possibility of the effect of SB431542 on both CAFs and HSC-3 cells.

Next, we investigated the role of SOX9 in cancer invasion using two different siRNAs for SOX9 knockdown in HSC-3 cells (Fig. 3E). Histological analysis showed that the invasion ability of SOX9-knockdown HSC-3 cells in the 3D HSC-3-CAF model was inhibited, despite the presence of CAFs, compared with HSC-3 cells treated with negative control siRNA or Lipofectamine alone (Fig. 3F). We confirmed that positive signals for SOX9 were decreased in SOX9-knockdown cells. In addition, both the depth of invasion and the invasion index were markedly suppressed in SOX9-knockdown cells (Fig. 3G and H).

Moreover, we examined the effect of CAFs on tumour growth and the involvement of the TGF-β/SOX9 axis in mouse xenograft models using HSC-3 and Ca9-22 cells. Both OSCC cell lines developed larger tumours with CAFs than those with NOFs (Fig 4A and B). Treatment with SB431542 suppressed tumour growth in mice inoculated with OSCC cells with CAFs (Fig 4A and B). No metastasis in other organs was observed in all mice. Histological analysis showed that the cancer-CAF tumours were composed of irregular, trabecular nests with desmoplastic stroma. The cancer-NOF tumours were small masses with a smooth margin (Fig. 4C and D). SOX9 expression was increased in the cancer-CAF tumours and α-SMA-positive stromal cells were detected in the stroma surrounding invasive nests. SOX9-positive OSCC cells at the invasive front showed an EMT-like phenotype characterised by decreased expression of E-cadherin and increased expression of vimentin (Fig. 4E). Furthermore, SOX9 expression was downregulated in cancer-CAF tumours treated with SB431542 (Fig. 4C and D). These *in vitro* and *in vivo* findings indicate that TGF-β-mediated invasion affects SOX9 expression in part and the TGF-β/SOX9 axis could play an important role in cancer invasion.

The presence of α-SMA-positive CAFs is correlated with SOX9 positivity in cancer nests and poor clinical outcome

We next investigated the localisation of CAFs and the expression patterns of SOX9 and TGF-β1 in human surgical specimens comprising 43 foci of normal epithelium, 48 foci of OED, 52 foci of CIS, and 65 foci of OSCC (Supplementary Table S1). Consistent with the previous report by Luksic et al. [12], the stromal cells including vascular smooth muscle cells and/or some fibroblasts were positive for α-SMA in OSCC surgical specimens. We also found that α-SMA-positive CAFs were localised in OSCC lesions (Fig. 5A). As shown in Supplementary Table S1, α-SMA--positive fibroblasts in the stroma were not detected in all normal epithelium, OED, or CIS but were only present in the stroma of 32 foci (49%) of OSCC, indicating that α-SMA-positive CAFs are likely to represent a specific phenotype in OSCC lesions. Furthermore, fibroblasts and macrophages in the stroma were positive for TGF-β1. Such TGF-β1-positive macrophages were found in OSCC stroma and the connective tissues in normal mucosa, OED, and CIS. However, TGF-β1-positive fibroblasts were present only in the stroma of OSCC, and their distribution was similar to that of α-SMA-positive CAFs (Fig. 5A and B). Moreover, strong SOX9 signals in OSCC cells occurred frequently in the invasive cancer nests surrounded by the aforementioned stroma. SOX9-positive OSCC cells at the invasive front showed an EMT-like phenotype characterised by decreased expression of

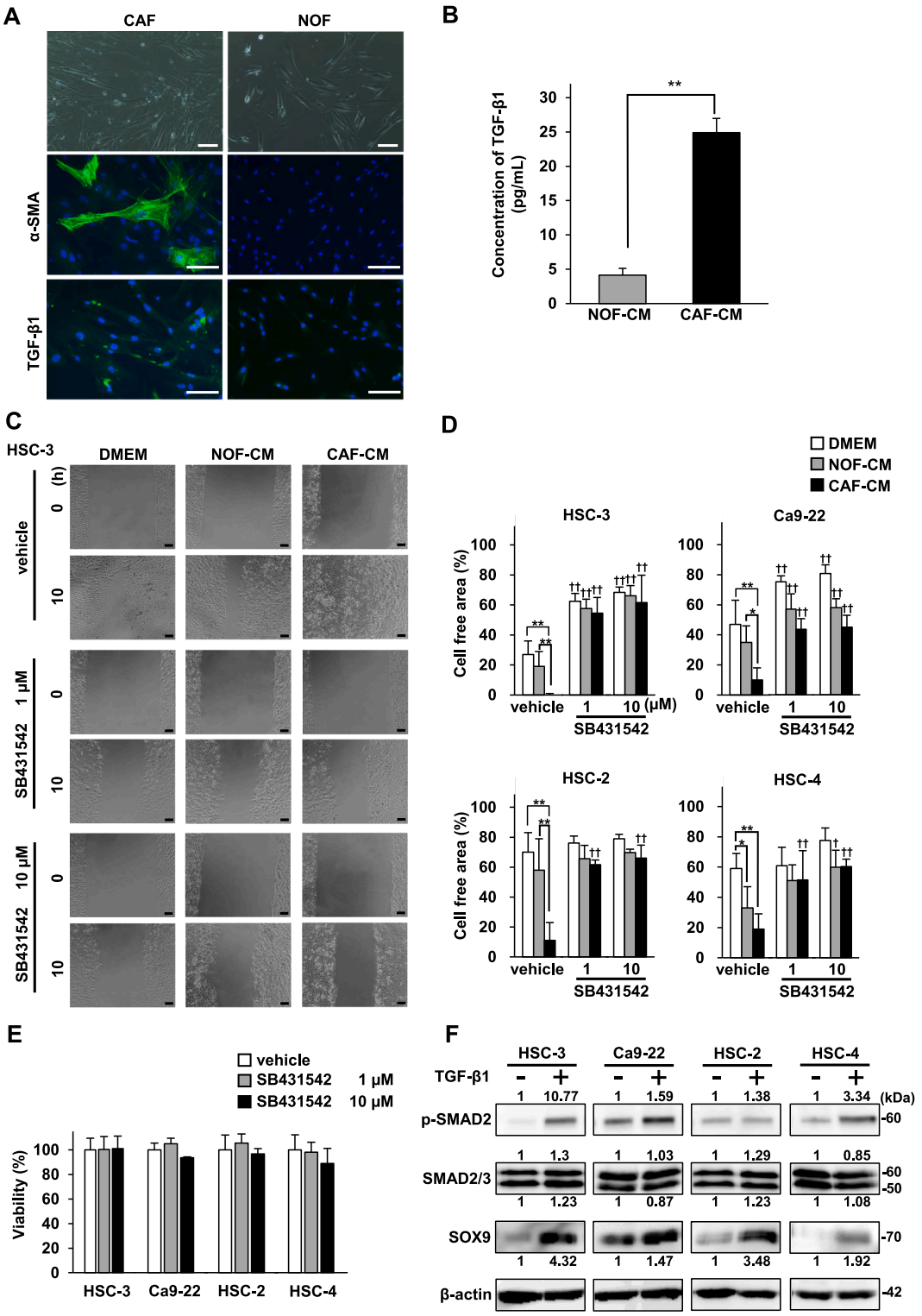

Fig. 1. CAF-derived TGF-β1 promotes the migration of OSCC cells, and TGF-β1 induces SOX9 expression in OSCC cells.
(A) The phase-contrast microscopic images and immunofluorescence staining of α-SMA and TGF-β1 in CAFs and NOFs. Green, α-SMA and TGF-β; blue, DAPI. Scale bars, 100 μm. (B) The concentration of TGF-β1 in NOF-CM and CAF-CM determined by ELISA. The concentrations represent the means ± *S*.D.; the experiments were run in triplicate and repeated three times. $^{**}p < 0.01$. (C) Representative images of the 2D migration assays. The four OSCC cell lines were incubated with DMEM, NOF-CM, or CAF-CM and treated with vehicle or SB431542 (1 μM or 10 μM). Representative images of only HSC-3 cells are shown. Scale bars, 100 μm. (D) Quantitative analysis of 2D migration assays. Bar graphs show the percentages of the wound closure areas of the four OSCC cell lines. The measurements were taken after 10 h for HSC-3 cells and 24 h for Ca9-22, HSC-2, and HSC-4 cells. The data represent the means ± *S*.D. ($n = 5$). $^{*}p < 0.05$, $^{**}p < 0.01$, compared with DMEM. $^{\dagger}p < 0.05$, $^{\dagger\dagger}p < 0.01$, compared with vehicle. (E) MTT cell viability assay of the four OSCC cell lines after treatment with vehicle or SB431542 (1 μM or 10 μM) for 24 h. The data represent the means ± *S*.D.; the experiments were run in triplicate and repeated three times. (F) Protein expression of SMAD signalling substrates and SOX9 in the four OSCC cell lines treated with or without TGF-β1 (10 ng/ml) for 48 h. Quantitative analyses of the proteins presented were carried out using ImageJ and were normalized with the loading control β-actin.

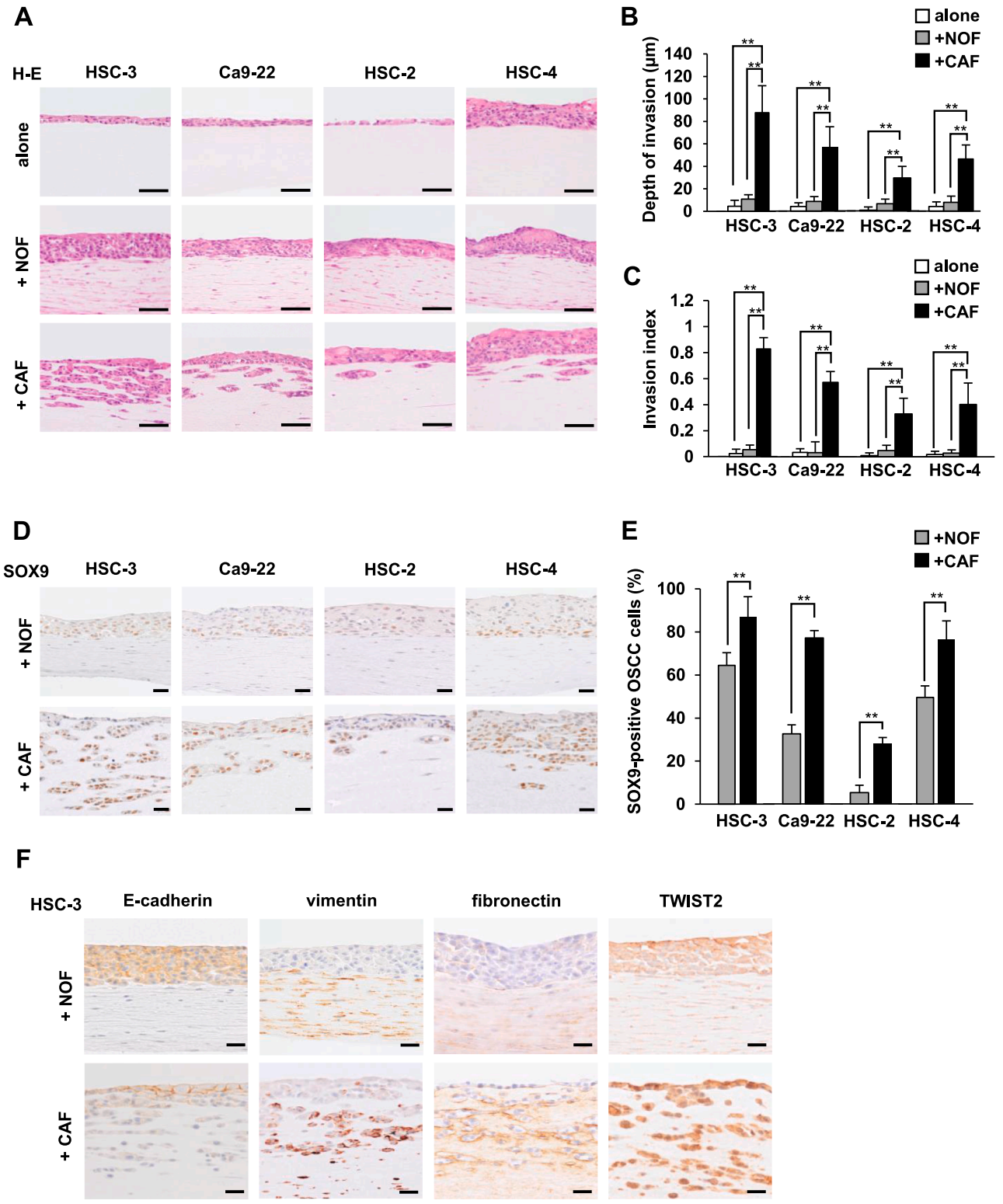

Fig. 2. CAFs promote cancer cell invasion in the 3D *in vitro* models, and SOX9 expression is enhanced in the invading cells with associated changes in the expression of EMT markers.

(A) Representative H-E staining of 3D cancer models consisting of four OSCC cell lines seeded on CAF- or NOF-embedded or acellular stromal layers. Scale bars, 50 μm. (B and C) Measurement of the depth of invasion (B) and the invasion index [1 − (non-invasive area/total area)] (C) in the 3D cancer models shown in (A). The data represent the means ± *S*.D. $^{**}p < 0.01$. (D) Representative immunohistochemical images of SOX9 in 3D cancer-NOF models and 3D cancer-CAF models. Scale bars, 20 μm. (E) The percentage of SOX9-positive OSCC cells in the 3D cancer-CAF and NOF models. The data represent the means ± *S*.D. of quintuplicate measurements. $^{**}p < 0.01$. (F) Representative immunohistochemical images of the EMT markers E-cadherin, vimentin, fibronectin, and TWIST2 in 3D HSC-3-NOF and 3D HSC-3-CAF models. Scale bars, 20 μm. 3D models were independently established and repeated three times.

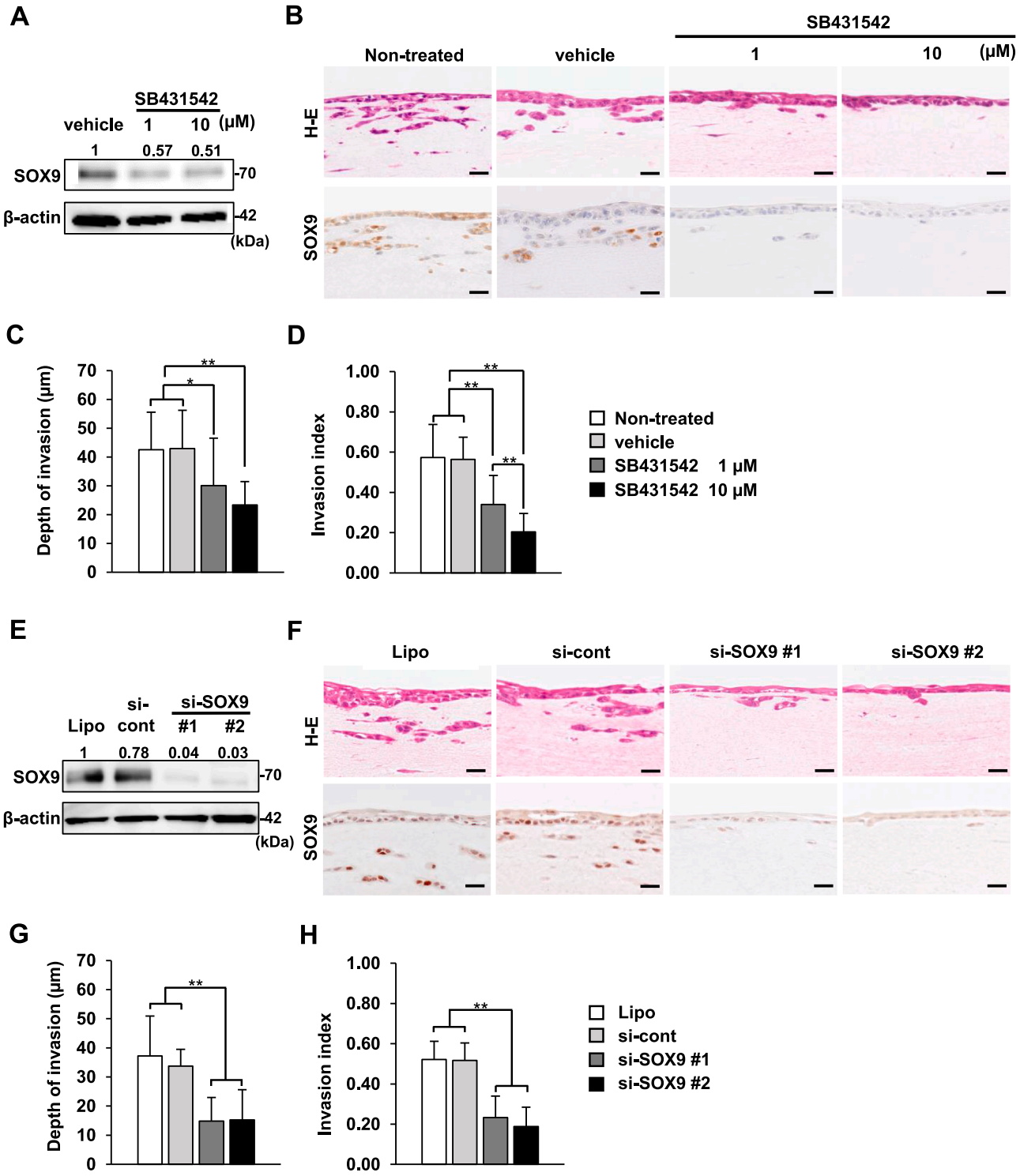

Fig. 3. Inhibition of TGF-β signalling and SOX9 knockdown decrease cancer invasion through downregulating SOX9 expression in the 3D HSC-3-CAF models. (A) Western blot analysis of SOX9 expression in HSC-3 cells treated with vehicle or SB431542 (1 μM or 10 μM) for 48 h. Quantitative analyses of the proteins presented were carried out using ImageJ and were normalised with the loading control β-actin. (B) Representative images of H-E staining and SOX9 immunohistochemistry in the 3D HSC-3-CAF model treated with vehicle or SB431542 (1 μM or 10 μM). For the control, the 3D HSC-3-CAF models were cultured with or without an equal volume of vehicle (dimethyl sulfoxide) (indicated as vehicle or non-treated, respectively). Scale bars, 20 μm. (C and D) Measurement of the depth of invasion (C) and the invasion index (D) of the 3D HSC-3-CAF model treated with SB431542. The data represent the means ± *S*.D. $*p < 0.05$, $**p < 0.01$. (E) Western blot analysis of SOX9 expression in HSC-3 cells transfected with SOX9-targeting siRNA or control siRNA (si-cont) using Lipofectamine or treated with Lipofectamine alone (Lipo). Quantitative analyses of the proteins presented were carried out using ImageJ and were normalized with the loading control β-actin. (F) Representative images of H-E staining and SOX9 immunohistochemistry in the 3D HSC-3-CAF model. HSC-3 cells were transfected with siRNA for SOX9 or si-cont or treated with Lipofectamine alone (Lipo). Scale bars, 20 μm. (G and H) Measurement of the depth of invasion (G) and the invasion index (H) in the 3D HSC-3-CAF model transfected with siRNA for SOX9 or si-cont using Lipofectamine or treated with Lipofectamine alone (Lipo). The data represent the means ± *S*.D. $**p < 0.01$. 3D models were independently established and repeated three times.

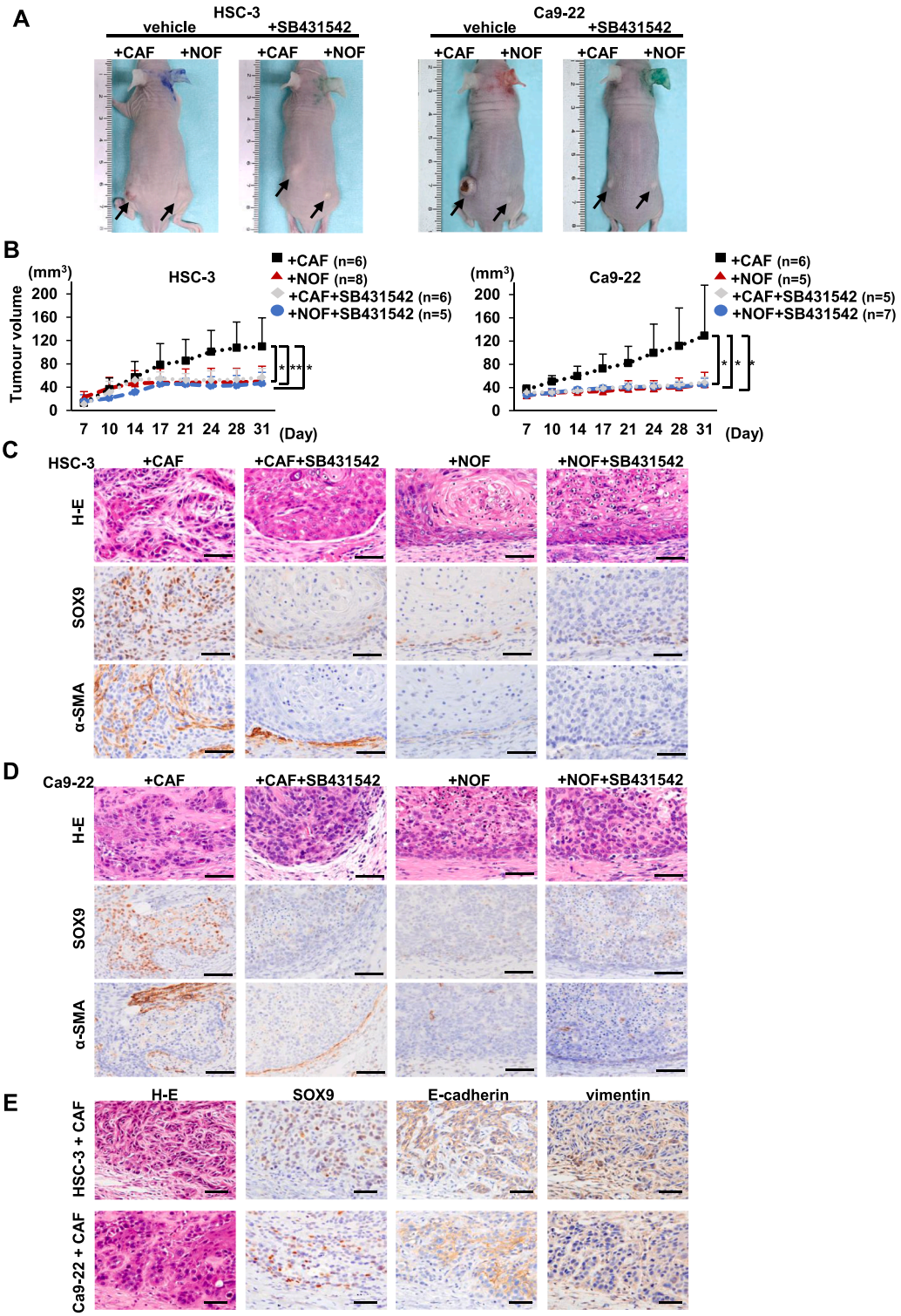

Fig. 4. CAFs promote tumour formation, and CAF-mediated tumour development is inhibited by SB431542 in mouse xenograft models.
(A) Representative macroscopic views of tumours formed in mouse xenograft models at 31 days after cell implantation with or without SB431542 treatment. OSCC cells (HSC-3 or Ca9-22 Cells) mixed with CAFs were implanted into the left flank and OSCC cells mixed with NOFs were implanted into the right flank. Mice were administered vehicle (dimethyl sulfoxide) or 10 mg/kg/mouse of SB431542. Arrows indicate tumours arising from implanted cells. (B) Tumour volume was measured twice a week starting at day 7 after inoculation. The data represent the means ± *S.D.* $^{*}p < 0.05$, $^{**}p < 0.01$. (C and D) Representative images of H-E staining and immunostaining for α-SMA and SOX9 in the tumours derived from HSC-3 (C) or Ca9-22 cells (D) mixed with CAFs or NOFs in mice treated with dimethyl sulfoxide or SB431542. Scale bars, 50 μm. (E) Representative images of H-E staining and immunohistochemistry for SOX9, E-cadherin, and vimentin in tumour xenografts derived from HSC-3 (upper) and Ca9-22 cells (lower) mixed with CAFs in mice. Scale bars, 50 μm.

E-cadherin and increased expression of vimentin (Fig. 5C), as well as in the mouse xenograft models.

The correlation of α-SMA-positive CAFs with clinicopathological characteristics is summarised in Table 1. The presence of α-SMA-positive CAFs in the cancer stroma was significantly correlated with the score of the mode of invasion ($p < 0.01$), SOX9 positivity in cancer nests ($p < 0.01$) and regional recurrence ($p < 0.05$). Moreover, as previously shown [18], high expression of SOX9 was also associated with regional recurrence ($p < 0.05$) (data not shown). In the survival analysis, the presence of α-SMA-positive CAFs was significantly correlated with relapse-free survival ($p < 0.01$), but was not significantly correlated with disease-specific survival ($p = 0.06$) (Fig. 5D and E).

Discussion

TGF-β is widely expressed and has functions as a strong extracellular signal that regulates EMT in cancer cells [29,30]. The TGF-β/SMAD pathway reportedly activated SOX9 in human cancers, such as lung

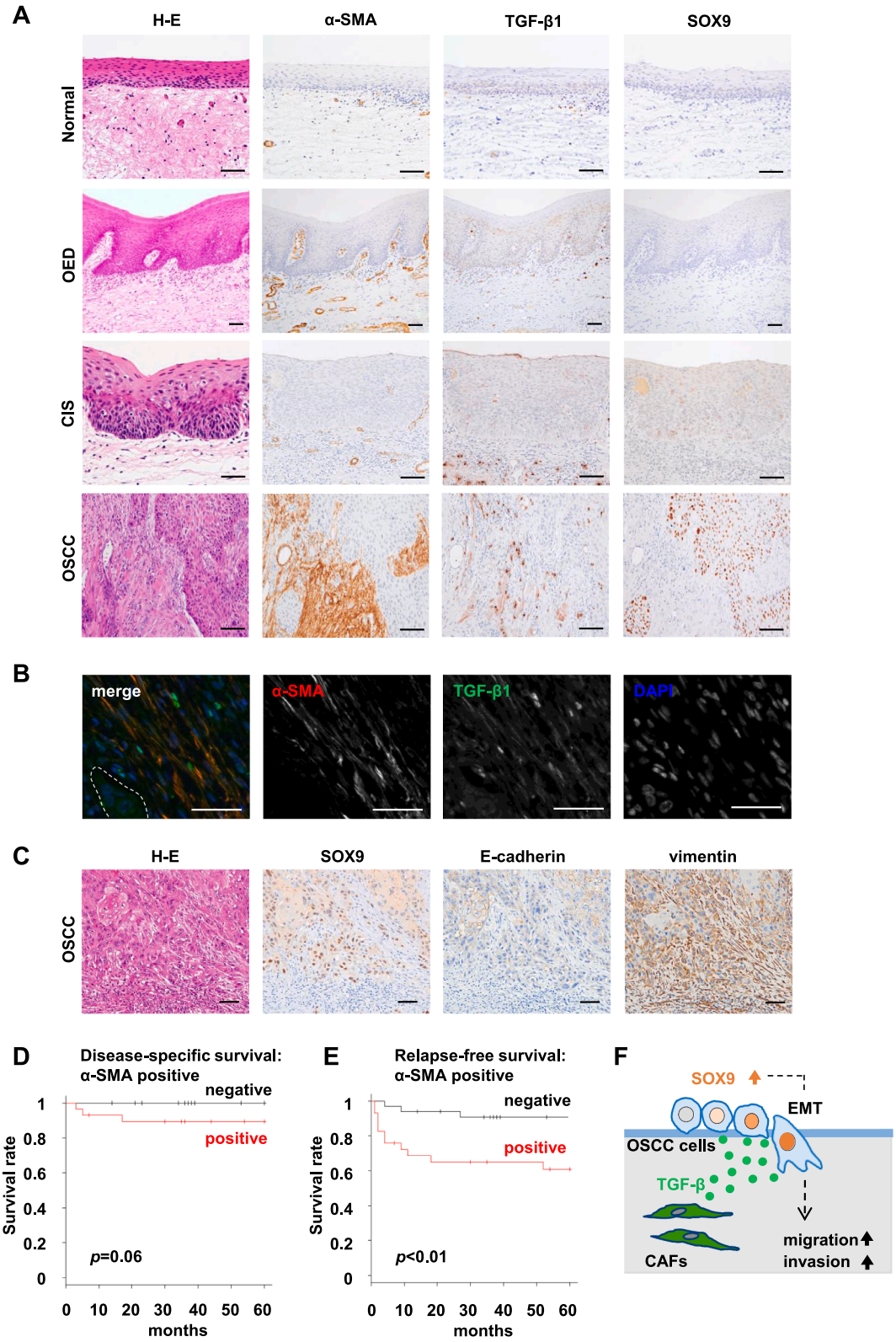

Fig. 5. SOX9 is strongly expressed in OSCC cells in the invasive cancer nests surrounded by α-SMA-positive CAFs, and α-SMA expression in cancer stroma are correlated with relapse-free survival.

(A) Representative images of H-E staining and immunostaining for α-SMA, SOX9, and TGF-β1 in normal, oral epithelial dysplasia (OED), carcinoma in situ (CIS), and oral squamous cell carcinoma (OSCC). Scale bars, 50 μm. (B) Double immunofluorescence staining of α-SMA and TGF-β1 in the stroma of OSCC. Red, α-SMA; green, TGF-β; blue, DAPI. The dotted area shows the cancer cell nests. Scale bars, 50 μm. (C) Representative images of H-E staining and immunohistochemistry for SOX9, E-cadherin, and vimentin in human OSCC tissues. Scale bars, 50 μm. (D and E) Kaplan–Meier curves showing disease-specific survival (D) and relapse-free survival (E) of patients with OSCC according to α-SMA expression in cancer stroma. The presence of α-SMA-positive fibroblasts was significantly associated with relapse-free survival ($p < 0.01$). (F) Schematic of the model from the present study. TGF-β secreted from CAFs may have significant roles in promoting the migration and invasion of OSCC cells via upregulating SOX9 expression that could induce EMT in OSCC cells.

Table 1
Relationship between the clinicopathological features of the OSCC cases and α-SMA expression in the stromal fibroblasts.

Characteristic	N	α-SMA expression, n (%)		*p*-value
		Positive	Negative	
Age				
≤ Median (72 years)	33	13 (39)	20 (61)	0.14
> Median	32	19 (59)	13 (41)	
Gender				
Male	36	15 (42)	21 (58)	0.22
Female	29	17 (59)	12 (41)	
T factor				
T1	22	8 (36)	14 (64)	0.05
T2	34	16 (47)	18 (53)	
T3	7	6 (86)	1 (14)	
T4	2	2 (100)	0 (0)	
Primary site				
Tongue	59	29 (49)	30 (51)	0.36
Buccal mucosa	4	3 (75)	1 (25)	
Gingiva	2	0 (0)	2 (100)	
Lymph node metastasis				
Negative	59	27 (46)	32 (54)	0.11
Positive	6	5 (83)	1 (17)	
Clinical stage				
I	22	8 (36)	14 (64)	0.05
II	31	14 (45)	17 (55)	
III	9	7 (78)	2 (22)	
IV	3	3 (100)	0 (0)	
Mode of invasion				
1	5	0 (0)	5 (100)	< 0.01
2	12	2 (17)	10 (83)	
3	27	12 (44)	15 (56)	
4	21	18 (86)	3 (14)	
SOX9 expression in OSCC cells				
Negative	26	6 (23)	20 (77)	< 0.01
Positive	39	26 (67)	13 (33)	
Local recurrence				
No	62	30 (48)	32 (52)	0.61
Yes	3	2 (67)	1 (33)	
Regional recurrence				
No	52	22 (42)	30 (58)	<0.05
Yes	13	10 (77)	3 (23)	

OSCC, oral squamous cell carcinoma; α-SMA, alpha-smooth muscle actin; SOX9, sex-determining region Y (SRY)-box9.

cancer [15], gastric cancer [30], and oesophageal adenocarcinoma [31]. We previously showed that SOX9 expression represents a potential predictive biomarker for cancer aggressiveness and a poor prognostic factor for OSCC [18]. Therefore, we investigated the mechanism regulating SOX9 expression in OSCC. On the basis of the hypothesis that TGF-β secreted by CAFs promotes cancer progression through the upregulation of SOX9 expression in OSCC cells, we investigated whether the TGF-β/SOX9 axis facilitates interactions between CAFs and cancer cells. This study demonstrates that CAFs promote cancer migration and invasion by inducing EMT in OSCC cells, and that the TGF-β/SOX9 axis contribute to the invasiveness (Fig. 5F).

Paracrine communication between CAFs and cancer cells plays a significant role in mediating cancer cell migration, invasion, and metastasis [7]. TGF-β is a pleiotropic cytokine that has an important role in maintaining epithelial homoeostasis. TGF-β suppresses tumour progression in normal epithelial and premalignant cells; however, dysfunctional TGF-β signalling frequently results in tumour development [32]. TGF-β1 is generally stored as a latent form in the TME and can be activated by plasmin, matrix metalloproteinase (MMP)-2, MMP-9, thrombospondin-1, lower pH, reactive oxygen species, and specific integrins [33]. As CAFs also secrete MMP-2 and MMP-9 [34], CAFs might contribute to activate TGF-β1. The loss of adaptor protein β-2 spectrin (β2SP) switches TGF-β function from tumour suppression to tumour promotion and activates SOX9 expression [31]. The present study clearly showed that CAFs have a more potent capacity to secrete TGF-β1 compared with NOFs, and CAF-induced TGF-β1 upregulates SOX9 expression in OSCC cells through the paracrine TGF-β signalling pathway and promotes cancer migration and invasion *in vitro* and *in vivo*.

We demonstrated that SOX9 plays an important role in the induction of EMT and invasion in OSCC. CAFs facilitate cancer migration and invasion by inducing the EMT in cancer cells through a paracrine TGF-β signalling pathway [35–37]. During cancer progression, SOX9 drives EMT through deubiquitination of Snail [38] and in cooperation with Slug [39] and TWIST [40]. SOX9 knockdown inhibits cell proliferation, whereas SOX9 overexpression inhibits apoptosis and increases cell proliferation in lung cancer [41]. The invading OSCC cells in our 3D *in vitro* models exhibited strong SOX9 expression with associated changes in the expression of EMT markers. Pharmacological inhibition of TGF-β signalling and knockdown of SOX9 drastically reduced cancer invasion, suggesting that TGF-β-mediated invasion is dependent on SOX9 expression. Therefore, the TGF-β/SOX9 axis may modulate cancer migration and invasion induced by EMT.

Histopathological investigations using OSCC surgical specimens revealed that the emergence of α-SMA-positive fibroblasts may be a useful marker for cancer invasion and poor clinical outcome. TGF-β [42], IL-1β [43], and leukaemia inhibitory factor [44] were shown to be potential promoters to transform resident fibroblasts into the CAF phenotype. An early event in carcinogenesis is the generation of activated fibroblasts or CAFs, which facilitate a breach of the basement membrane [45]. Cancer stromal fibroblasts, which are continuously exposed to different stimuli in the TME, are induced by cancer cells to secrete excessive and abnormal soluble factors and modify the stromal ECM. The fibroblasts then undergo changes in their properties as CAFs [7]. The current study showed that α-SMA expression is only localised to the stromal fibroblasts of OSCC and not to the normal epithelium, OED, or CIS. Taken together, our results suggest that switching from normal fibroblasts to α-SMA-positive CAFs might occur in the steps before and after the invasion. Recent studies have indicated that CAF subtypes might be determined depending on their differential tumour-promoting capability [46], and α-SMA-positive CAFs are considered cancer-promoting CAFs [47]. Therefore, CAFs may be present in early OED lesions; however, they may be undetectable by α-SMA immunohistochemistry. Further investigation is required to establish more specific markers of CAFs in early OSCC for the early detection of carcinogenesis.

We also showed that the structure of our 3D *in vitro* models mimicked biomimetic materials suitable for studying the TME, in which CAFs, NOFs, or no cells resided in the collagen matrix as “stromal tissue” and OSCC cells were overlaid as “parenchymal tissue”. Recently, several useful 3D *in vitro* models have emerged for the evaluation of CAF–cancer cell interactions [8,44,48], and a cell–sheet 3D cancer model was assessed for chemotherapeutic screening [49]. The 3D cancer-CAF models described in the current study enable histological and immunohistological examinations of early invasive cancer, and identify the properties of cancer cells were consistent with those of human cancers.

This study had several limitations. We used CAFs obtained from lung cancer to develop 3D cancer-CAF models, because stable isolation of CAFs from oral cancer had not yet been established. The use of commercially available CAFs derived from lung cancer can reduce the variation in characteristics among cells. We used these cells to perform the experiments, which could be readily repeated to confirm reproducibility. However, CAFs obtained from lung cancer and oral cancer may have different characteristics regarding cancer progression. Therefore, further studies are necessary to elucidate the interaction between CAFs and cancer cells in OSCC using CAFs obtained from patients with OSCC.

In conclusion, our results indicate that TGF-β1 secreted from CAFs plays a significant role in promoting the migration and invasion of OSCC cells via upregulating SOX9 expression that could induce EMT. Blocking this pathway could be a potential novel therapeutic strategy for patients with OSCC.

CRediT authorship contribution statement

Kenta Haga: Conceptualization, Methodology, Formal analysis, Investigation, Resources, Writing – original draft, Writing – review & editing, Visualization. **Manabu Yamazaki:** Conceptualization, Methodology, Formal analysis, Investigation, Data curation, Writing – original draft, Writing – review & editing, Visualization, Supervision. **Satoshi Maruyama:** Formal analysis, Investigation, Writing – review & editing. **Masami Kawaharada:** Investigation, Writing – review & editing. **Ayako Suzuki:** Investigation, Resources, Writing – review & editing. **Emi Hoshikawa:** Investigation, Resources, Data curation, Writing – review & editing. **Nyein Nyein Chan:** Investigation, Writing – review & editing. **Akinori Funayama:** Writing – review & editing, Funding acquisition. **Toshihiko Mikami:** Writing – review & editing, Funding acquisition. **Tadaharu Kobayashi:** Conceptualization, Methodology, Writing – review & editing, Supervision, Project administration, Funding acquisition. **Kenji Izumi:** Conceptualization, Methodology, Formal analysis, Writing – review & editing, Project administration. **Jun-ichi Tanuma:** Conceptualization, Methodology, Formal analysis, Investigation, Writing – review & editing, Supervision, Project administration, Funding acquisition.

Declaration of Competing Interest

The authors declare no potential conflicts of interest.

Data accessibility

The data underlying this article will be shared on reasonable request to the corresponding author.

Funding

The author(s) disclose receipt of the following financial support for the research, authorship, and/or publication of this article: This research was supported by Japan Society for the Promotion of Science KAKENHI Grant Number 19K10329 to A.F., 19K10354 to T.M., 18K09875 to T.K and 19K10069 to J-I.T.

Supplementary materials

Supplementary material associated with this article can be found, in the online version, at doi:10.1016/j.tranon.2021.101236.

References

[1] A.A. Hussein, M.N. Helder, J.G. Visscher, C.R. Leemans, B.J. Braakhuis, H.C.W. de Vet, T. Forouzanfar, Global incidence of oral and oropharynx cancer in patients younger than 45 years versus older patients: a systematic review, Eur. J. Cancer 82 (2017) 115–127, https://doi.org/10.1016/j.ejca.2017.05.026.

[2] F. Bray, J. Ferlay, I. Soerjomataram, R.L. Siegel, L.A. Torre, A. Jemal, Global cancer statistics 2018: GLOBOCAN estimates of incidence and mortality worldwide for 36 cancers in 185 countries, CA Cancer J. Clin. 68 (2018) 394–424, https://doi.org/10.3322/caac.21492.

[3] S. Yanamoto, H. Yamada, H. Takahashi, I. Yoshitomi, G. Kawasaki, H. Ikeda, T. Minamizato, T. Shiraishi, S. Fujita, T. Ikeda, I. Asahina, M. Umeda, Clinicopathological risk factors for local recurrence in oral squamous cell carcinoma, Int. J. Oral Maxillofac. Surg. 41 (2012) 1195–1200, https://doi.org/10.1016/j.ijom.2012.07.011.

[4] P.G. Arduino, M. Carrozzo, A. Chiecchio, R. Broccoletti, F. Tirone, E. Borra, G. Bertolusso, S. Gandolfo, Clinical and histopathologic independent prognostic factors in oral squamous cell carcinoma: a retrospective study of 334 cases, J. Oral Maxillofac. Surg. 66 (2008) 1570–1579, https://doi.org/10.1016/j.joms.2007.12.024.

[5] G. Lorusso, C. Rüegg, The tumor microenvironment and its contribution to tumor evolution toward metastasis, Histochem. Cell Biol. 130 (2008) 1091–1103, https://doi.org/10.1007/s00418-008-0530-8.

[6] A. Orimo, P.B. Gupta, D.C. Sgroi, F. Arenzana-Seisdedos, T. Delaunay, R. Naeem, V. J. Carey, A.L. Richardson, R.A. Wein-berg, Stromal fibroblasts present in invasive human breast carcinomas promote tumor growth and angiogenesis through elevated sdf-1/cxcl12 secretion, Cell 121 (2005) 335–348, https://doi.org/10.1016/j.cell.2005.02.034.

[7] B. Erdogan, D.J. Webb, Cancer-associated fibroblasts modulate growth factor signaling and extracellular matrix remodeling to regulate tumor metastasis, Biochem. Soc. Trans. 45 (2017) 229–236, https://doi.org/10.1042/BST20160387.

[8] C. Gaggioli, S. Hooper, C. Hidalgo-Carcedo, R. Grosse, J.F. Marshall, K. Harrington, E. Sahai, Fibroblast-led collective invasion of carcinoma cells with differing roles for RhoGTPases in leading and following cells, Nat. Cell Biol. 9 (2007) 1392–1400, https://doi.org/10.1038/ncb1658.

[9] Y. Yu, C.H. Xiao, L.D. Tan, Q.S. Wang, X.Q. Li, Y.M. Feng, Cancer-associated fibroblasts induce epithelial–mesenchymal transition of breast cancer cells through paracrine TGF-β signalling, Br. J. Cancer 110 (2014) 724–732, https://doi.org/10.1038/bjc.2013.768.

[10] T.A. Karakasheva, E.W. Lin, Q. Tang, E. Qiao, T.J. Waldron, M. Soni, A.J. Klein-Szanto, V. Sahu, D. Basu, S. Ohashi, K. Baba, Z.T. Giaccone, S.R. Walker, D. A. Frank, E.P. Wileyto, Q. Long, M.C. Dunagin, A. Raj, J.A. Diehl, K.K. Wong, A. J. Bass, A.K. Rustgi, IL-6 mediates cross-talk between tumor cells and activated fibroblasts in the tumor microenvironment, Cancer Res. 78 (2018) 4957–4970, https://doi.org/10.1158/0008-5472.CAN-17-2268.

[11] R. Kalluri, M. Zeisberg, Fibroblasts in cancer, Nat. Rev. Cancer 6 (2006) 392–401, https://doi.org/10.1038/nrc1877.

[12] I. Luksic, P. Suton, S. Manojlovic, M. Virag, M. Petrovecki, D. Macan, Significance of myofibroblast appearance in squamous cell carcinoma of the oral cavity on the occurrence of occult regional metastases, distant metastases, and survival, Int. J. Oral Maxillofac. Surg. 44 (2015) 1075–1080, https://doi.org/10.1016/j.ijom.2015.05.009.

[13] M. Sinn, C. Denkert, J.K. Striefler, U. Pelzer, J.M. Stieler, M. Bahra, P. Lohneis, B. Dörken, H. Oettle, H. Riess, B.V. Sinn, α-Smooth muscle actin expression and desmoplastic stromal reaction in pancreatic cancer: results from the CONKO-001 study, Br. J. Cancer 111 (2014) 1917–1923, https://doi.org/10.1038/bjc.2014.495.

[14] V. Lefebvre, B. Dumitriu, A. Penzo-Meńdez, Y. Han, B. Pallavi, Control of cell fate and differentiation by Sry-related high-mobility-group box (Sox) transcription factors, Int. J. Biochem. Cell Biol. 39 (2007) 2195–2214, https://doi.org/10.1016/j.biocel.2007.05.019.

[15] S. Zhang, D. Che, F. Yang, C. Chi, H. Meng, J. Shen, L. Qi, F. Liu, L. Lv, Y. Li, Q. Meng, J. Liu, L. Shang, Y. Yu, Tu-mor-associated macrophages promote tumor metastasis via the TGF-β/SOX9 axis in non-small cell lung cancer, Oncotarget 8 (2017) 99801–99815, https://doi.org/10.1007/s00418-008-0530-8.

[16] N. Higo, H. Okumura, Y. Uchikado, I. Omoto, K. Sasaki, Y. Kita, D. Ryosuke, M. Noda, T. Owaki, S. Ishigami, S. Natsugoe, Expression of SOX9 is related to prognosis in patients with squamous cell carcinoma, In Vivo 32 (2018) 835–838, https://doi.org/10.21873/invivo.11316 (Brooklyn).

[17] Y.P. Wan, M. Xi, H.C. He, S. Wan, W. Hua, Z.C. Zen, Y.L. Liu, Y.L. Zhou, R.J. Mo, Y. J. Zhuo, H.W. Luo, F.N. Jiang, W.D. Zhong, Expression and clinical significance of SOX9 in renal cell carcinoma, bladder cancer and penile cancer, Oncol. Res. Treat. 40 (2017) 15–20, https://doi.org/10.1159/000455145.

[18] Y. Sumita, M. Yamazaki, S. Maruyama, T. Abe, J. Cheng, R. Takagi, J.I. Tanuma, Cytoplasmic expression of SOX9 as a poor prognostic factor for oral squamous cell carcinoma, Oncol. Rep. 40 (2018) 2487–2496, https://doi.org/10.3892/or.2018.6665.

[19] Y. Imamura, T. Mukohara, Y. Shimono, Y. Funakoshi, N. Chayahara, M. Toyoda, N. Kiyota, S. Takao, S. Kono, T. Nakatsura, H. Minami, Comparison of 2D- and 3D-culture models as drug-testing platforms in breast cancer, Oncol. Rep. 33 (2015) 1837–1843, https://doi.org/10.3892/or.2015.3767.

[20] A.S. Nunes, A.S. Barros, E.C. Costa, A.F. Moreira, I.J. Correia, 3D tumor spheroids as in vitro models to mimic *in vivo* human solid tumors resistance to therapeutic drugs, Biotechnol. Bioeng. 116 (2019) 206–226, https://doi.org/10.1002/bit.26845.

[21] A. Shiomi, K. Izumi, A. Uenoyama, T. Saito, N. Saito, H. Ohnuki, H. Kato, M. Kanatani, S. Nomura, H. Egusa, T. Maeda, Cyclic mechanical pressure-loading alters epithelial homeostasis in a three-dimensional in vitro oral mucosa model: clinical implications for denture-wearers, J. Oral Rehabil. 42 (2015) 192–201, https://doi.org/10.1111/joor.12254.

[22] M. Horikoshi, Y. Kimura, H. Nagura, T. Ono, H. Ito, A new human cell line derived from human carcinoma of the gingiva. I its establishment and morphological studies, Jpn. J. Oral Maxillofac. Surg. 20 (1974) 100–106, https://doi.org/10.5794/jjoms.20.100.

[23] F. Momose, S. Hirata, T. Nitta, N. Tanaka, S. Shiota, The properties of three oral squamous cell carcinoma-derived cells, J. Jpn. Stomatol. Soc. 35 (1986) 485–496, https://doi.org/10.11277/stomatology1952.35.485.

[24] J.D. Brierley, M.K. Gospodarowicz, C. Wittekind, TNM Classification of Malignant Tumors, eds, 8th Ed., Wiley Blackwell, New Jersey, 2017, pp. 17–21.

[25] P.A. Jakobsson, C.M. Eneroth, D. Killander, G. Moberger, B. Martensson, Histologic classification and grading of malignancy in carcinoma of the larynx, Acta Radiol. Ther. Phys. Biol. 12 (1973) 1–8, https://doi.org/10.3109/02841867309131085.

[26] J. Cheng, T. Irié, R. Munakata, S. Kimura, H. Nakamura, R.G. He, A.R. Liu, T. Saku, Biosynthesis of basement membrane molecules by salivary adenoid cystic carcinoma cells: an immunofluorescence and confocal microscopic study, Virchows Ach 426 (1995) 577–586, https://doi.org/10.1007/BF00192112.

[27] M. Yamazaki, S. Maruyama, T. Abé, M. Tsuneki, H. Kato, K. Izumi, J.I. Tanuma, J. Cheng, T. Saku, Rac1-dependent phagocytosis of apoptotic cells by oral squamous cell carcinoma cells: a possible driving force for tumor progression, Exp. Cell Res. 392 (2020), 112013, https://doi.org/10.1016/j.yexcr.2020.112013.

[28] S. Nurmenniemi, T. Sinikumpu, I. Alahuhta, S. Salo, M. Sutinen, M. Santala, J. Risteli, P. Nyberg, T. Salo, A novel organotypic model mimics the tumor microenvironment, Am. J. Pathol. 175 (2009) 1281–1291, https://doi.org/10.2353/ajpath.2009.081110.

[29] J.Q. Bu, F. Chen, TGF-β1 promotes cells invasion and migration by inducing epithelial mesenchymal transformation in oral squamous cell carcinoma, Eur. Rev. Med. Pharmacol. Sci. 21 (2017) 2137–2144.
[30] T.H.Huang Li, G. Shi, L. Zhao, T. Li, Z. Zhang, R. Liu, Y. Hu, H. Liu, J. Yu, G. Li, TGF-β1-SOX9 axis-inducible COL10A1 promotes invasion and metastasis in gastric cancer via epithelial-to-mesenchymal transition, Cell Death Dis. 9 (2018) 849, https://doi.org/10.1038/s41419-018-0877-2.
[31] S. Song, D.M. Maru, J.A. Ajani, C.H. Chan, S. Honjo, H.K. Lin, A. Correa, W. L. Hofstetter, M. Davila, J. Stroehlein, L. Mishra, Loss of TGF-β adaptor β2SP activates notch signaling and SOX9 expression in esophageal adenocarcinoma, Cancer Res. 73 (2013) 2159–2169, https://doi.org/10.1158/0008-5472.CAN-12-1962.
[32] J. Massagué, TGFβ in Cancer, Cell 134 (2008) 215–230, https://doi.org/10.1016/j.cell.2008.07.001.
[33] X. Xu, L. Zheng, Q. Yuan, G. Zhen, J.L. Crane, X. Zhou, X. Cao, Transforming growth factor-β in stem cells and tissue homeostasis, Bone Res. 6 (2) (2018), https://doi.org/10.1038/s41413-017-0005-4.
[34] S. Koontongkaew, P. Amornphimoltham, P. Monthanpisut, T. Saensuk, M. Leelakriangsak, Fibroblasts and extracellular matrix differently modulate MMP activation by primary and metastatic head and neck cancer cells, Med. Oncol. 2 (2012) 690–703, https://doi.org/10.1007/s12032-011-9871-6.
[35] J. Zhuang, Q. Lu, B. Shen, X. Huang, L. Shen, X. Zheng, R. Huang, J. Yan, H. Guo, TGFβ1 secreted by cancer associated fibroblasts induces epithelial-mesenchymal transition of bladder cancer cells through lncRNA-ZEB2, Sci. Rep. 5 (2015) 11924, https://doi.org/10.1038/srep11924.
[36] Y. Ren, H.H. Jia, Y.Q. Xu, X. Zhou, X.H. Zhao, Y.F. Wang, X. Song, Z.Y. Zhu, T. Sun, Y. Dou, W.P. Tian, X.L. Zhao, C.S. Kang, M. Mei, Paracrine and epigenetic control of CAF-induced metastasis: the role of HOTAIR stimulated by TGF-β1 secretion, Mol. Cancer 17 (2018) 5, https://doi.org/10.1186/s12943-018-0758-4.
[37] Y. Yu, C.H. Xiao, L.D. Tan, Q.S. Wang, X.Q. Li, Y.M. Feng, Cancer-associated fibroblasts induce epithelial-mesenchymal transition of breast cancer cells through paracrine TGF-β signaling, Br. J. Cancer 110 (2014) 724–732, https://doi.org/10.1038/bjc.2013.768.
[38] B.J. Choi, S.A. Park, S.Y. Lee, Y.N. Cha, Y.J. Surh, Hypoxia induces epithelial-mesenchymal transition in colorectal cancer cells through ubiquitin-specific protease 47-mediated stabilization of Snail: a potential role of Sox9, Sci. Rep. 7 (2017) 15918, https://doi.org/10.1038/s41598-017-15139-5.
[39] W. Guo, Z. Keckesova, J.L. Donaher, T. Shibue, V. Tischler, F. Reinhardt, S. Itzkovitz, A. Noske, U. Zürrer-Härdi, G. Bell, W.L. Tam, S.A. Mani, A. van Oudenaarden, R.A. Weinberg, Slug and Sox9 cooperatively determine the mammary stem cell state, Cell 148 (2012) 1015–1028, https://doi.org/10.1016/j.cell.2012.02.008.
[40] S.S.N. Lam, C.K.M. Ip, A.S.C. Mak, A.S.T. Wong, A novel p70 S6 kinase-microRNA biogenesis axis mediates multicellular spheroid formation in ovarian cancer progression, Oncotarget 7 (2016) 38064–38077, https://doi.org/10.18632/oncotarget.9345.
[41] G. Coricor, R. Serra, TGF-β regulates phosphorylation and stabilization of Sox9 protein in chondrocytes through p38 and Smad dependent mechanisms, Sci. Rep. 6 (2016) 38616, https://doi.org/10.1038/srep38616.
[42] M.P. Lewis, K.A. Lygoe, M.L. Nystrom, W.P. Anderson, P.M. Speight, J.F. Marshall, G.J. Thomas, Tumour-derived TGF-β1 modulates myofibroblast differentiation and promotes HGF/SF-dependent invasion of squamous carcinoma cells, Br. J. Cancer 90 (2004) 822–832, https://doi.org/10.1038/sj.bjc.6601611.
[43] J. Dudás, A. Fullára, M. Bitsche, V. Schartinger, I. Kovalszky, G.M. Sprinzl, H. Riechelmann, Tumor-produced, active Interleukin-1 β regulates gene expression in carcinoma-associated fibroblasts, Exp. Cell Res. 317 (2011) 2222–2229, https://doi.org/10.1016/j.yexcr.2011.05.023.
[44] J. Albrengues, T. Bertero, E. Grasset, S. Bonan, M. Maiel, I. Bourget, C. Philippe, C. H. Serrano, S. Benamar, O. Croce, V. Sanz-Moreno, G. Meneguzzi, C.C. Feral, G. Cristofari, C. Gaggioli, Epigenetic switch drives the conversion of fibroblasts into proinvasive cancer-associated fibroblasts, Nat. Commun. 6 (2015) 10204, https://doi.org/10.1038/ncomms10204.
[45] A. Glentis, P. Oertle, P. Mariani, A. Chikina, E.F. Marjou, Y. Attieh, F. Zaccarini, M. Lae, D. Loew, F. Dingli, P. Sirven, M. Schoumacher, B.G. Gurchenkov, M. Plodinec, D.M. Vignjevic, Cancer-associated fibroblasts induce metalloprotease-independent cancer cell invasion of the basement membrane, Nat. Commun. 8 (2017) 924, https://doi.org/10.1038/s41467-017-00985-8.
[46] D.E. Costea, A. Hills, A.H. Osman, J. Thurlow, G. Kalna, X. Huang, P.C. Murillo, H. Parajuli, S. Suliman, K.K. Kulasekara, A.C. Johannessen, M. Partridge, Identification of two distinct carcinoma-associated fibroblast subtypes with differential tumor-promoting abilities in oral squamous cell carcinoma, Cancer Res. 73 (2013) 3888–3902, https://doi.org/10.1158/0008-5472.CAN-12-4150.
[47] Y. Mizutani, H. Kobayashi, T. Iida, N. Asai, A. Masamune, A. Hara, N. Esaki, K. Ushida, S. Mii, Y. Shiraki, K. Ando, L. Weng, S. Ishihara, S.M. Ponik, M. W. Conklin, H. Haga, A. Nagasaka, T. Miyata, M. Matsuyama, T. Kobayashi, T. Fujii, S. Yamada, J. Yamaguchi, T. Wang, S.L. Woods, D. Worthley, T. Shimamura, M. Fujishiro, Y. Hirooka, A. Enomoto, M. Takahashi, Meflin-positive cancer-associated fibroblasts inhibit pancreatic carcinogenesis, Cancer Res. 79 (2019) 5367–5381, https://doi.org/10.1158/0008-5472.CAN-19-0454.
[48] S.A. Kim, E.K. Lee, H.J. Kuh, Co-culture of 3D tumor spheroids with fibroblasts as a model for epithelial-mesenchymal transition in vitro, Exp. Cell Res. 335 (2015) 187–196, https://doi.org/10.1016/j.yexcr.2015.05.016.
[49] J. Lee, D. Shin, J.L. Roh, Development of an in vitro cell-sheet cancer model for chemotherapeutic screening, Theranostics 8 (2018) 3964–3973, https://doi.org/10.7150/thno.26439.